

Improving of Asphalt Pavement Performance using Steel wire Grid Reinforcement

Ahmed Mohamady¹, Abu-Bakr M. Elhady² and Mohamed S. Eisa³

¹Assoc. Prof. of Highways and Airports Engineering, Faculty of Engineering Zagazig University

²Egyptian Space Program

³Ph. D Candidate, Faculty of Engineering Zagazig University.

¹dr_a_mohamady@yahoo.com, ²amelhady@netscape.net and ³mohamedeisa524@yahoo.com

Abstract: This study aims to investigate the effect of using steel wire grid reinforcement on the performance of pavement sections. The reinforced pavement sections are modeled and analyzed using two-dimensional finite elements method. Study was using the ADINA finite element program. In this study three paving sections were analyzed. The first section represents one of the commonly sections used in the paving of local roads, the second section is commonly used in expressways and the third section is used in freeways. The reinforcement was arranged at different depths. Steel wire grid reinforced sections results are compared to geosynthetics grid reinforced sections as well as typical rigid pavement section commonly used in Egypt. The analysis showed that the best location of reinforcement is at bottom of base layer in all investigated pavement sections. Comparisons show that steel mesh reinforced sections performance improved than geosynthetics grid reinforced sections and almost close to rigid section.

Keywords: Pavement, Steel wire grid, Two-dimensional Finite elements, ADINA and Geosynthetics grid

I. INTRODUCTION

Recently high axle loads were used the highway network as a result of high quantities of goods. Also several locations of low speeds were introduced due to high traffic volumes. All of these and other may cause pavement deformations. The deformation may be noticed as a pavement distresses. The most famous distresses are rutting, sags, corrugations, cracking, etc. Pavement distresses cause many troubles to the vehicles and users [1,2]. The maintenance of such distresses may need high budget and time consuming and hence cause traffic troubles during maintenance and repair processes. The design of flexible pavements is largely based on empirical methods. However, there is currently a shift underway towards more mechanistic design techniques. Layered elastic analysis and two-dimensional finite element (FE) methods have been generally been used to determine stresses, strains and displacements in flexible pavement [3-5].

There are many commercially available reinforcement products (such as steel mesh, glass fiber grid, carbon fiber web, etc.) are used to control reflective cracking and/or increase rutting resistance [6,7]. However, due to the many factors influencing function and performance of reinforcement products, it is extremely difficult to predict their field performance. A recent release of the American Association of Highway and Transportation Officials (AASHTO 2001) provides a recommended practice guide for geosynthetic reinforcement incorporation in the flexible pavement system. However, such a guide is not intended for addressing the structural benefits offered by the addition of a geosynthetic reinforcement layer. Evaluating the benefits added to the flexible pavement system as a consequence of using the reinforcement geosynthetic has been the objective of several new research projects, which have been initiated in the United States [8].

II. OBJECTIVES AND METHODOLOGY

This study conducted on paving sections used in places that have vehicles to reduce speed as a result of traffic and the presence of some speed sedatives like railway crossing and town entrances also at places of U-turns to opposite directions. This study also aims to strengthen the pavement layers of these sections with steel wire grid or geosynthetics grid at different depths and effect of this strengthen to reduce the stresses on the pavement sections and hence increasing the pavement life. Three paving sections were studied; section A, B and C represents local roads, expressways and freeways respectively. The proposed layers thicknesses and the associated properties for the investigated sections are shown in table (1) [10,11]. These sections rested on infinite subgrade soil and its modulus of elasticity is 50 MPa and value of poisson's ratio is 0.25. The reinforcement materials are steel wire grid or geosynthetics grid with wire diameter 4mm and square cell side length 10cm and its properties were given in table (2)[6,7].

The locations of strengthening in section A were chosen at bottom of wearing surface, middle of base and bottom of base, while in section B the locations of strengthening were chosen at bottom of wearing

surface, bottom of binder layer, middle of base and bottom of base, finally the locations of strengthening in section C were chosen at bottom of wearing surface, bottom of binder layer, bottom of bituminous base, middle of base and bottom of base. The reinforced sections were compared with typical rigid pavement section commonly used in Egypt to evaluate the proposed strengthening technique.

III. FINITE ELEMENTS MODEL (FEM)

Considering the studied sections are modeled as multilayer semi finite elements. All materials are treated as homogeneous and isotropic. Deformations are considered very small relative to the dimensions so the equation of liner elasticity is valid.

3.1 Finite element computer package ADINA

The multi-purpose finite element program ADINA version 8.7 [9] was used to model 2-D finite element analysis. All asphalt layers was modeled as 2D-solid elements as 8- node plane strain elements, with two translational degrees of freedom per node. This type of node gives a high level of accuracy in combination with an acceptable computing time demand. The steel reinforcement was modeled as truss element and defined with the area steel of selected number and diameter of the reinforcement grid.

3.2 Kinematic and kinetic boundary conditions

The boundary conditions and loading of static analysis for selected sections are shown in fig (1). It can be observed that the bottom of the pavement is fixed at Y and Z translations while the sides of pavement are restricted with Y translation only.

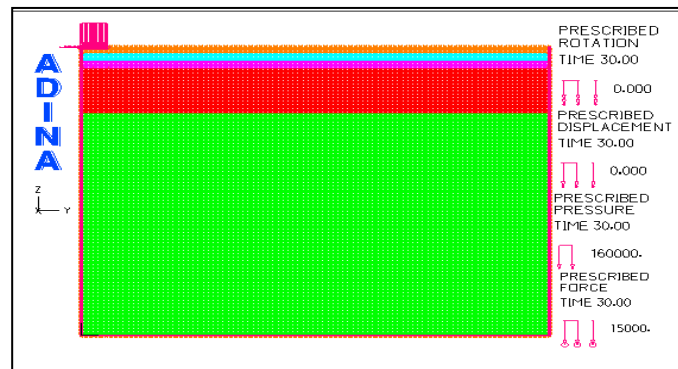


Fig. (1) FEM model for sec(C)

IV. RESULTS AND DISCUSSION

The most important parameters in pavement design are lateral tensile strain and vertical compressive stress as shown in fig (2).The investigated cases were modelled with ADINA program and the results were presented and discussed here in after.

4.1 Analysis of sections subject to vertical loads

4.1.1 Lateral strain

For sections A, B and C the lateral strain ϵ_Y variation versus section depth under center of wheel pressure are presented in figures (3) to (8). Figures present comparison of lateral strain variation in sections Without and with reinforcement at different depths.

Table (1): Layers thickness and the associated properties for the investigated sections

Section	Layer	Modulus of elasticity (Mpa)	Passion's ratio	Density (KN/m ³)	Thickness (mm)
A	Wearing surface	2757.91	0.30	22.00	50
	Base	275.791	0.20	20.00	300
B	Wearing surface	2757.91	0.30	22.00	50
	Binder	2757.91	0.30	22.00	50
	Base	275.791	0.20	20.00	400
	Wearing surface	2757.91	0.30	22.00	50

C	Binder	2757.91	0.30	22.00	60
	Bituminous base	2413.16	0.35	21.00	70
	Base	275.791	0.20	20.00	400

Table (2): The properties of reinforcing materials

Material	Modulus of elasticity (Mpa)	Passion's ratio	Density (KN/m ³)
Steel	210000	0.25	78.50
Geosynthetics	4230	0.35	18.00

It is depicted that for the case without reinforcement the lateral strain starts with negative value at top of wearing surface layer and rapidly increases to zero approximately at middle of wearing surface layer then continue increases to the maximum value at bottom of base layer and vanished at the end of section. The maximum lateral strain ϵ_y values at bottom of base layers in sections A, B and C are 4.27E-04, 3.13E-04 and 2.54E-04 respectively. For reinforced section the lateral strain behavior the same as unreinforced sections but it is confined at the reinforcement location Figures (3) and (4) for section (A) show when we add the steel reinforcement at the middle of base layer the lateral strain ϵ_y is decreased to 3.86E-05 i.e. decreasing percent is 80.35% from without reinforcement case (1.96E-04) then arrived to 3.24E-04 at bottom of base layer i.e. 24.12% decreasing percent from the strain in original case. Figures also illustrate that there is a drastic change the lateral strain ϵ_y values when the steel reinforcement at bottom of base layer, lateral strain ϵ_y in this location was 5.67E-05 i.e. decreasing percent is 86.70% from its value in without reinforcement case. While in case of reinforcement with geosynthetic at same location the lateral strain ϵ_y was 3.58E-04 i.e. decreasing percent is 16.00% from its value in without reinforcement case. Also show there are no change in lateral strain ϵ_y distribution for others cases and case without reinforcement.

Figures (5) and (6) for section (B) explain that there is no change in the strain values in cases of steel or geosynthetic reinforcement at bottom of wearing surface, at bottom of binder layer and geosynthetic reinforcement at middle of base layer, shows that there is a noticeable change in case steel reinforcement at middle of base layer. In this location the lateral strain ϵ_y is decreased to 3.75E-05 i.e. decreasing percent is 77.5% from without reinforcement case (1.67E-04) then arrived to 2.30E-04 at bottom of base layer i.e. 26.6% decreasing percent from the lateral strain ϵ_y in original case. Figures also illustrate that there is a drastic change in the lateral strain ϵ_y values when the steel reinforcement at bottom of base layer, lateral strain ϵ_y in this location was 5.13E-05 i.e. decreasing percent is 83.60% from its value in without reinforcement case. While in case of reinforcement with geosynthetic at same location lateral strain ϵ_y was 2.74E-04 i.e. decreasing percent is 12.55% from its value in without reinforcement case.

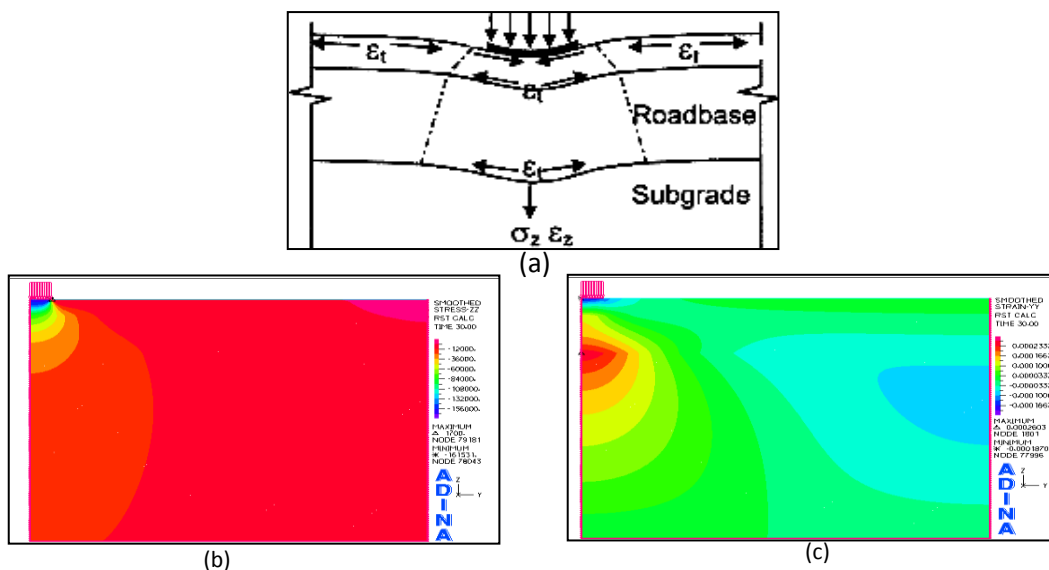


Fig. (2): (a) Response of a flexible pavement under wheel load (b) Vertical stress σ_z (c) Lateral strain ϵ_y

Figures (7) and (8) for section (C) illustrate that there is a noticeable change when we add the steel reinforcement at middle of base layer, the lateral strain ϵ_Y is decreased to $4.31E-05$ i.e. 72.01% decreasing percent from without reinforcement case ($1.54E-04$) then arrived to $1.69E-04$ at bottom of base layer i.e. 33.30% decreasing percent from the strain in ordinary case. And illustrate that there is a drastic change in lateral strain ϵ_Y values when the steel reinforcement was at bottom of base layer. The lateral strain ϵ_Y arrived in this location to $4.69E-05$ i.e. decreasing percent is 81.50% from its value in without reinforcement case. While for case of reinforcement with geosythetic the lateral strain ϵ_Y arrived in this location to $2.27E-04$ i.e. decreasing percent is 10.62% from its value in without reinforcement case. Figures show that there is no change in lateral strain ϵ_Y distribution in others cases and case without reinforcement.

4.1.2 Vertical stress

Figures (9) to (14) present the variation of vertical stress σ_Z at bottom of base layer in sections A, B and C due to vertical pressure of wheel and illustrate the effect of adding reinforcement with different locations. Figures (9) and (10) for section (A) exhibit that the vertical stress σ_Z in without reinforcement case start decrease from $-4.82E+04$ Pa under the center line of the wheel load to zero Pa at the surface, and shows that there is no change in cases reinforcement at bottom of wearing surface. Figures also show that there is a noticeable change when steel reinforcement was arranged at middle of base layer, the vertical stress σ_Z under the center line of the wheel load decreased to $-4.63+04$ Pa i.e.19% from without reinforcement case, while for case of reinforcement with geosythetic there is no change. Figures illustrate that there is a drastic change in vertical stress σ_Z values when the steel reinforcement was added at bottom of base layer, the vertical stress σ_Z under the center line of the wheel load decreased to $-2.51+04$ Pa i.e.48% from without reinforcement case, while in case of reinforcement with geosythetic arrived to $-3.10+04$ Pa i.e.35.6% from without reinforcement case.

Figures (13) and (14) for section (C) explain that the vertical stress σ_Z in without reinforcement case start decrease from $-2.84E+04$ Pa under the center line of the wheel load to zero Pa at the surface. Figures show that there is no change in cases reinforcement at bottom of wearing surface, bottom of binder layer and bottom of bituminous base layer. Figures also show that there is a noticeable change when we add the steel reinforcement at middle of base layer, in this location vertical stress σ_Z under the center line of the wheel load decreased to $-2.61+04$ Pa i.e. 8% from without reinforcement case while for case of reinforcement with geosythetic there is no change. Figures illustrate that there is a drastic change in vertical stress σ_Z values when the reinforcement was at bottom of base layer, vertical stress σ_Z under the center line of the wheel load decreased to $-1.48+04$ Pa i.e.48% from without reinforcement case, while in case of reinforcement with geosythetic arrived to $-1.85+04$ Pa i.e.35% from without reinforcement case.

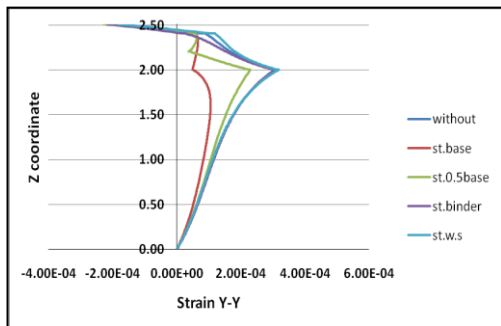


Fig. (3) Lateral strain ϵ_Y due to vertical pressure of wheel versus section depth for section (A) with and without steel reinforcement

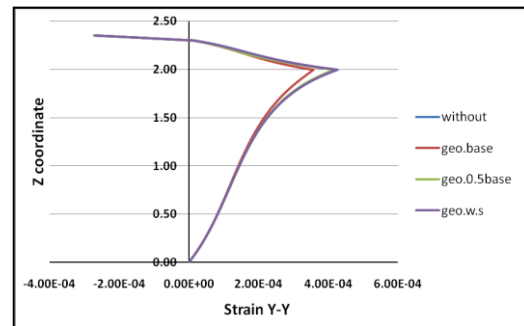


Fig. (4) Lateral strain ϵ_Y due to vertical pressure of wheel versus section depth for section (A) with and without geosynthetics reinforcement

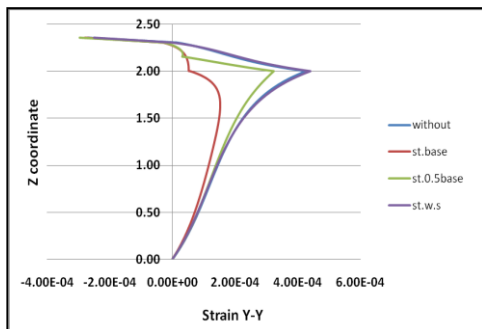


Fig. (5) Lateral strain ϵ_Y due to vertical pressure of wheel versus section depth for se. (B) with and without steel reinforcement

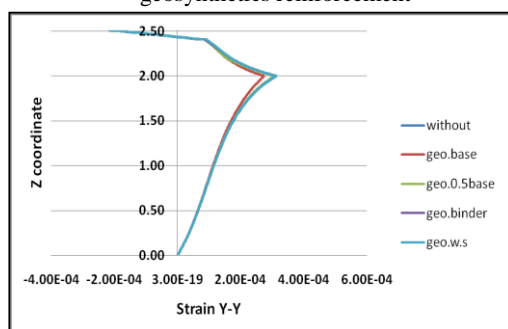


Fig. (6) Lateral strain ϵ_Y due to vertical pressure of wheel versus section depth for sec. (B) with and without geosynthetics reinforcement

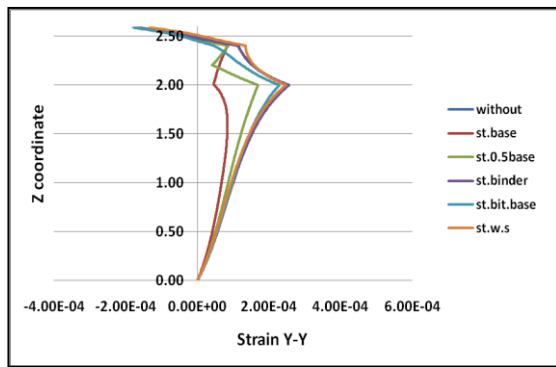


Fig. (7) Lateral strain ϵ_Y due to vertical pressure of wheel versus section depth for sec. (C) with and without steel reinforcement

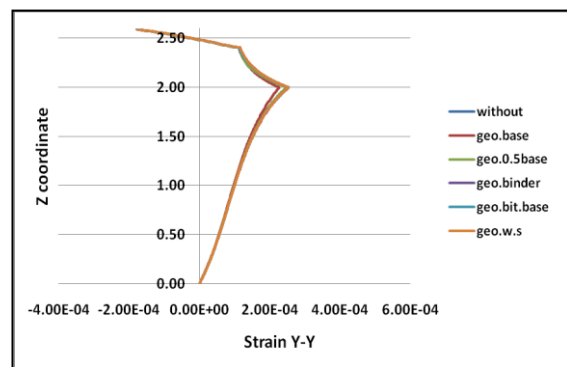


Fig. (8) Lateral strain ϵ_Y due to vertical pressure of wheel versus section depth for sec. (C) with and without geosynthetics reinforcement

4.2 Analysis of sections subject to vertical loads and friction force

4.2.1 Lateral strain

Figures (15) to (20) present the variation of lateral strain under the center line of the wheel through the depth of the sections A, B and C due to vertical pressure of wheel and horizontal friction force. Figures (15) and (16) for section (A) clarify that in without reinforcement case the lateral strain ϵ_Y start increase from $1.93E-04$ at surface to $3.00E-04$ at bottom of wearing surface layer then decrease to $1.87E-04$ at 160mm from the surface then increase to $3.14E-04$ at bottom of base layer and then decreases to decay. But for steel reinforcement at middle of base layer the lateral strain ϵ_Y start increase from $1.50E-04$ at surface to $2.44E-04$ at 60mm from surface then decrease to $4.45E-05$ at middle of base then increase to $1.81E-04$ i.e. 42.35% of ordinary value at bottom of base layer then decreases to decay. Figures also show the lateral strain ϵ_Y in geosynthetic reinforcement at bottom of base layer decreased by 10.8% from values in without reinforcement case. And for steel reinforcement the lateral strain ϵ_Y start increase from $1.71E-04$ at surface to $2.52E-04$ at 60mm from surface then decrease to $5.27E-05$ at bottom of base layer i.e. decreasing percent is 83.60% from its value in without reinforcement case and then decreases to decay.

Figures (17) and (18) for section (B) show that in without reinforcement case the horizontal lateral strain ϵ_Y start increase from $1.60E-04$ at surface to $1.66E-04$ at 20mm from surface layer then decrease to $9.61E-05$ at 180mm from surface layer then increase to $2.32E-04$ at bottom of base layer then decreases to decay. Figures show in case steel reinforcement at bottom of wearing surface layer the lateral strain ϵ_Y start increase from $8.57E-05$ at surface to $9.04E-05$ at 10mm from surface then decrease to $5.37E-05$ at 50mm from surface layer then increase to $2.43E-04$ at surface of sub grade and then decreases to decay. Figures also show in case of steel reinforcement at bottom of binder layer the lateral strain ϵ_Y start increase from $1.23E-04$ at surface to $1.27E-04$ at 10mm from surface then decrease to $4.31E-05$ at 160mm from surface layer then increase to $2.09E-04$ i.e. 10% of original case at surface of sub grade and then decreases to decay. Figures also show in case of steel reinforcement at middle of base layer the lateral strain ϵ_Y start increase from $1.44E-04$ at surface to $1.49E-04$ at 10mm from surface then decrease to $3.48E-05$ at 250mm from surface layer then increase to $1.44E-04$ i.e. 37.9% of ordinary value at surface of sub grade and then decreases to decay. Figures also illustrates that no change in the lateral strain ϵ_Y values between adding the geosynthetic reinforcement at bottom of base layer and the case without reinforcement from surface to subgrade but the lateral strain ϵ_Y at surface of subgrade decreased by 10.8% from the lateral strain ϵ_Y in without reinforcement case. And for steel reinforcement the lateral strain ϵ_Y start increase from $1.61E-04$ at surface to $1.64E-04$ at 10mm from surface then decrease to $3.86E-05$ at 290 mm from surface layer then increased to $4.44E-05$ i.e. 80.75% of ordinary value at bottom of base layer and then decreases to decay. Figures show that there is no change in lateral strain ϵ_Y distribution in others cases and the case without reinforcement.

Figures (11) and (12) for section (B) display that in without reinforcement case the vertical stress σ_Z start decrease from $-3.43E+04$ Pa under the center line of the wheel load to zero Pa at the surface, and show that there is no change in cases reinforcement at bottom of wearing surface, at bottom of binder layer. Figures also show that there is a noticeable change when the steel reinforcement was arranged at middle of base layer, in this location the vertical stress σ_Z under the center line of the wheel load decreased to $-3.25+04$ Pa i.e. 18% from without reinforcement case, while for case of reinforcement with geosynthetic there is no change. Figures also illustrate that there is a drastic change in vertical stress σ_Z values when the steel reinforcement was added at bottom of base layer. The vertical stress σ_Z under the center line of the wheel load decreased to $-1.78+04$ Pa i.e. 48% from without reinforcement case. In case of reinforcement with geosynthetic arrived to $-2.22+04$ Pa i.e. 35.50% from without reinforcement case.

Figures (19) and (20) for section (C) display that in without reinforcement case the lateral strain ϵ_Y start increase from $1.29E-04$ at surface to $1.35E-04$ at 20mm from surface layer then decrease to $6.07E-05$ at 190mm from surface layer then increase to $1.85E-04$ at bottom of base layer and then decreases to decay. For steel reinforcement at bottom of wearing surface the lateral strain ϵ_Y start increase from $6.96E-05$ at surface to $7.52E-05$ at 10mm from surface then decrease to $4.03E-05$ at 50mm from surface layer then increase to $1.97E-04$ at bottom of base layer and then decreases to decay. In case of steel at bottom of binder layer the lateral strain ϵ_Y start increase from $1.12E-04$ at surface to $1.17E-04$ at 10mm from surface then decrease to $4.31E-05$ at 110mm from surface layer then increase to $1.83E-04$ at bottom of base layer and then decreases to decay. Figures show in case steel reinforcement at bottom of bituminous base layer the lateral strain ϵ_Y start increase from $1.10E-04$ at surface to $1.15E-04$ at 20mm from surface then decrease to $3.60E-05$ at 190mm from surface layer then increase to $1.56E-04$ i.e. 16% of ordinary value at bottom of base layer and then decreases to decay. Figures also present that no change in the lateral strain ϵ_Y values between adding the geosynthetic reinforcement at the middle of base layer and the case without reinforcement from surface to subgrade but the lateral strain ϵ_Y at surface of subgrade decreased by 10.8% from the lateral strain ϵ_Y in without reinforcement case, while for steel reinforcement at the same location the lateral strain ϵ_Y start increase from $1.25E-04$ at surface to $1.29E-04$ at 10mm from surface then decrease to $3.12E-05$ at 250mm from surface layer then increase to $1.07E-04$ i.e. 42.16% of ordinary value at bottom of base layer and then decreases to decay. Figures also illustrate that no change in the lateral strain ϵ_Y values between adding the geosynthetic reinforcement at bottom of base layer and the case without reinforcement from surface to subgrade But the lateral strain ϵ_Y at surface of subgrade decreased by 8% from the lateral strain ϵ_Y in without reinforcement case, while for steel reinforcement the lateral strain ϵ_Y start increase from $1.38E-04$ at surface to $1.42E-04$ at 10mm from surface then decrease to $3.86E-05$ at 170 mm from surface layer then increased to $4.03E-05$ i.e. 78.30% of ordinary value at bottom of base layer and then decreases to decay. Figures show that there is no change in lateral strain ϵ_Y distribution in others cases and the case without reinforcement.

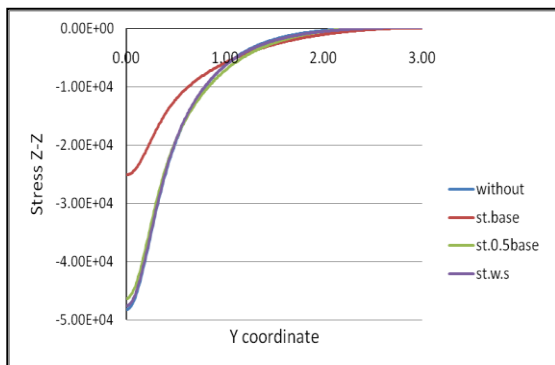


Fig. (9) Vertical stress σ_z due to vertical pressure of wheel at bottom of base layer for sec. (A) with and without steel reinforcement

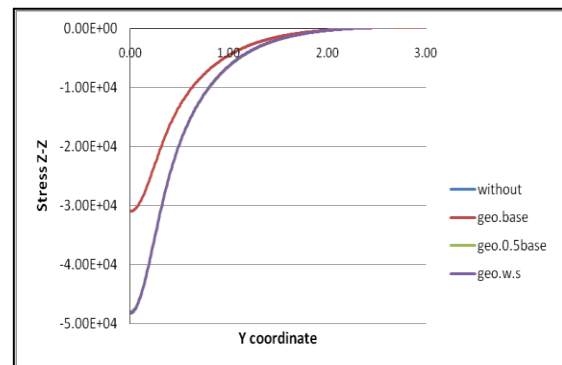


Fig. (10) Vertical stress σ_z due to vertical pressure of wheel at bottom of base layer for sec. (A) with and without geosynthetic reinforcement

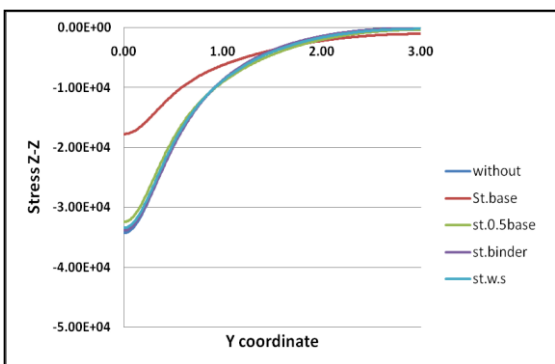


Fig. (11) Vertical stress σ_z due to vertical pressure of wheel at bottom of base layer for sec. (B) with and without steel reinforcement

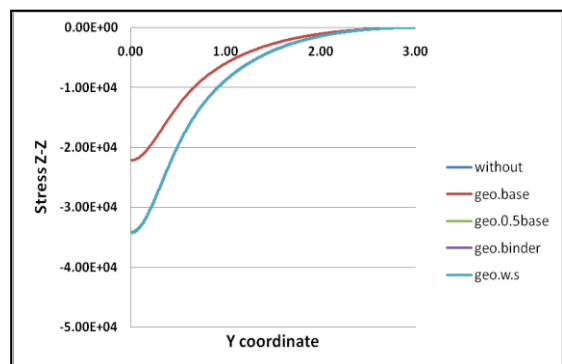


Fig. (12) Vertical stress σ_z due to vertical pressure of wheel at bottom of base layer for sec. (B) with and without geosynthetic reinforcement

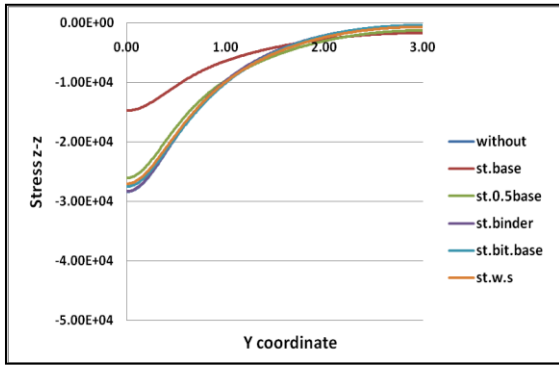


Fig. (13) Vertical stress σ_z due to vertical pressure of wheel at bottom of base layer for sec. (C) with and without steel reinforcement

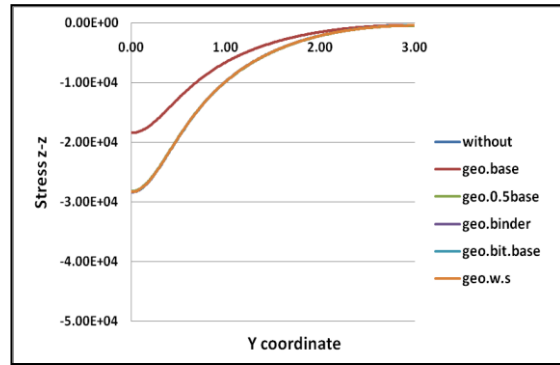


Fig. (14) Vertical stress σ_z due to vertical pressure of wheel at bottom of base layer for sec. (C) with and without geosynthetic reinforcement

4.2.2 Vertical stress

Figures (21) to (26) present the variation of vertical stress σ_z at bottom of base layer in sections A, B and C due to vertical pressure of wheel and horizontal force subject to friction and illustrate the effect of adding reinforcement with different locations.

Figures (21) and (22) for section (A) show that the vertical stress σ_z in without reinforcement case start increase from $-3.48E+04$ Pa under the center line of the wheel load to $-3.61E+04$ Pa at 0.17 m from center line of the wheel load and then decreases to decay at the end of section width. Figures also show that there is no change in cases reinforcement at bottom of wearing surface. Figures also show that there is a noticeable change when we add the steel reinforcement at middle of base layer, the vertical stress σ_z start increase from $-3.17E+04$ Pa i.e. decrease percent is 8.9% under the center line of the wheel load to $-3.38E+04$ Pa i.e. decrease percent is 12.29% at 0.17 m from center line of the wheel load and then decreases to decay at the end of section width, while for case of reinforcement with geosynthetic there is no change. Figures illustrate that there is a drastic change in vertical stress σ_z values when the steel reinforcement was added at bottom of base layer, The vertical stress σ_z start increase from $-1.77E+04$ Pa i.e. decrease percent is 48.75% under the center line of the wheel load to $-1.86E+04$ Pa i.e. decrease percent is 48.47% at 0.17 m from center line of the wheel load and then decreases to decay at the end of section width, while in case of reinforcement with geosynthetic ,the vertical stress σ_z start increase from $-2.23E+04$ Pa i.e. decrease percent is 35.91% under the center line of the wheel load to $-2.33E+04$ Pa i.e. decrease percent is 35.45% at 0.17 m from center line of the wheel load and then decreases to decay at the end of section width.

Figures (23) and (24) for section (B) explain that in without reinforcement case the vertical stress σ_z start increase from $-2.72E+04$ Pa under the center line of the wheel load to $-2.73E+04$ Pa at 0.17 m from center line of the wheel load and then decreases to decay at the end of section width. Figures also show that there is a noticeable change when we add the steel reinforcement at middle of base layer, the vertical stress σ_z start increase from $-2.49E+04$ Pa i.e. decrease percent is 8.5% under the center line of the wheel load to $-2.51E+04$ Pa i.e. decrease percent is 8.29% at 0.20 m from center line of the wheel load and then decreases to decay at the end of section width.. Figures also illustrate that there is a drastic change in vertical stress σ_z values when the steel reinforcement was added at bottom of base layer, The vertical stress σ_z start from $-1.41E+04$ Pa i.e. decrease percent is 48.5% under the center line of the wheel load and still at same value to 0.17 m from center line of the wheel load and then decreases to decay at the end of section width, while in case of reinforcement with geosynthetic The vertical stress σ_z start from $-1.74E+04$ Pa i.e. decrease percent is 36% under the center line of the wheel load and still at same value to 0.17 m from center line of the wheel load and then decreases to decay at the end of section width. Figures show that there is no change in vertical stress σ_z distribution in others cases and the case without reinforcement.

Figures (25) and (26) for section (C) show that the vertical stress σ_z in without reinforcement case start from $-2.32E+04$ Pa under the center line of the wheel load and still at same value $-2.32E+04$ Pa at 0.17 m from center line of the wheel load and then decreases to decay at the end of section width. Figures also show that there is no change in cases reinforcement at bottom of wearing surface and at bottom of binder layer. Figures also show that there is a noticeable change when we add the steel reinforcement at the end of bituminous base layer, the vertical stress σ_z start from $-2.22E+04$ Pa i.e. decrease percent is 4.31% under the center line of the wheel load and still at same value to 0.17 m from center line of the wheel load and then decreases to decay at the end of section width, while there is no change in geosynthetic reinforcement at same location. Figures also show that there is a noticeable change when we add the steel reinforcement at middle of base layer, the vertical stress σ_z start from $-2.07E+04$ Pa i.e. decrease percent is 10.77% under the center line of the wheel load and still

at same value to 0.17 m from center line of the wheel load and then decreases to decay at end of section width. Figures also show that there is a drastic change in vertical stress σ_z values when the reinforcement was added at bottom of base layer. The vertical stress σ_z start from $-1.21E+04Pa$ i.e. decrease percent is 48% under the center line of the wheel load and still at same value to 0.17m from center line of the wheel load and then decreases to decay at end of section width, while in case of reinforcement with geosythetic, the vertical stress σ_z start from $-1.49E+04Pa$ i.e. decrease percent is 35.9% under the center line of the wheel load and still at same value to 0.17 m from center line of the wheel load and then decreases to decay at end of section width.

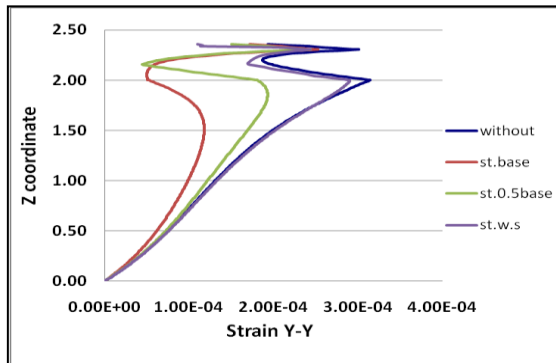


Fig. (15) Lateral strain ϵ_Y due to vertical pressure of wheel and friction force versus section depth for sec. (A) with and without steel reinforcement

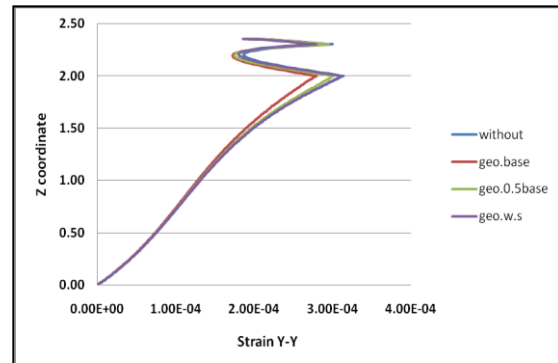


Fig. (16) Lateral strain ϵ_Y due to vertical pressure of wheel and friction force versus section depth for sec. (A) with and without geosynthetics reinforcement

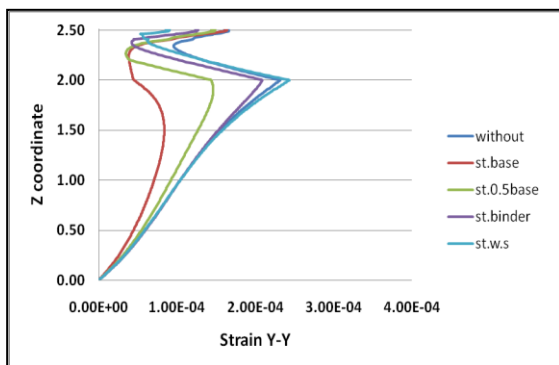


Fig. (17) Lateral strain ϵ_Y due to vertical pressure of wheel and friction force versus section depth for sec. (B) with and without steel reinforcement

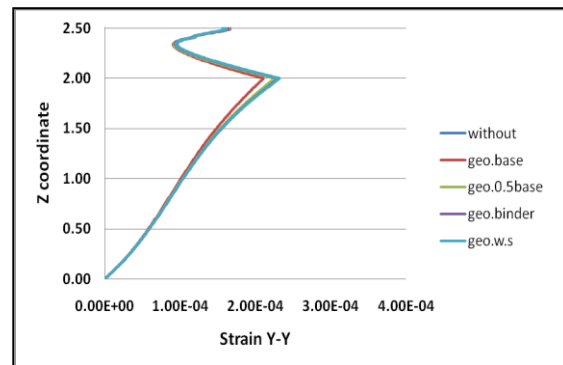


Fig. (18) Lateral strain ϵ_Y due to vertical pressure of wheel and friction force versus section depth for sec. (B) with and without geosynthetics reinforcement

4.3 Comparison between the reinforced flexible pavements sections and rigid pavement section

4.3.1 Vertical stress

Figures (27) and (28) present the variation of vertical stress σ_z at top of subgrade for paving sections (A), (B) and (C) with steel or geosynthetic reinforcement and selected rigid pavement section 20cm reinforced concrete slab with steel diameter is 8 mm and rested on 15cm sub base layer.

From figure (27) it is clear that the values of vertical stress σ_z in section reinforced with steel wire grid are lower than the values in section reinforced with geosynthetic. Figure (28) show that the value of vertical stress σ_z under the wheel in rigid pavement section is lower with 15.93% than value in section (A) reinforced with steel, but it is greater with 15.64% than values in sections (B) reinforced with steel and greater with 29.85% than the stress in section (C) reinforced with steel.

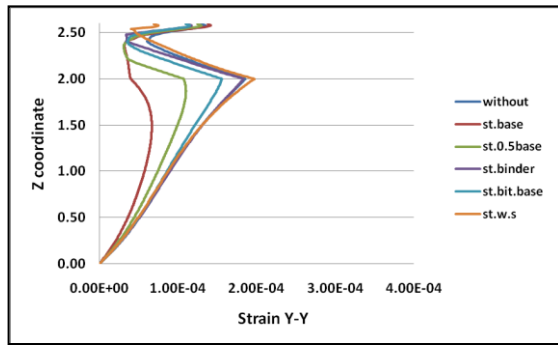


Fig. (19) Lateral strain ϵ_Y due to vertical pressure of wheel and friction force versus section depth for sec. (C) with and without steel reinforcement

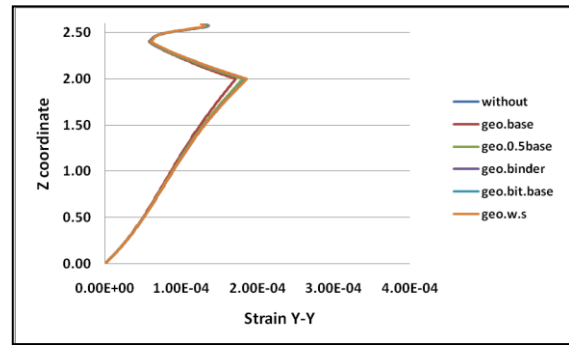


Fig. (20) Lateral strain ϵ_Y due to vertical pressure of wheel and friction force versus section depth for sec. (C) with and without geosynthetics reinforcement

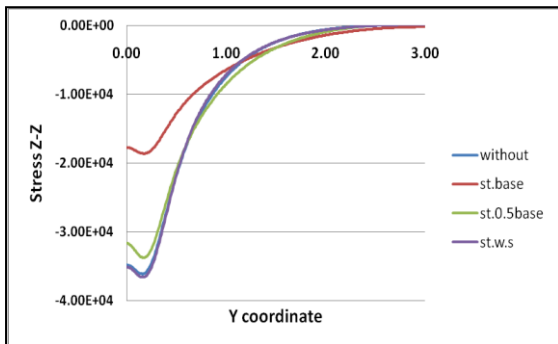


Fig. (21) Vertical stress σ_Z due to vertical pressure of wheel and friction force at bottom of base layer for sec. (A) with and without steel reinforcement

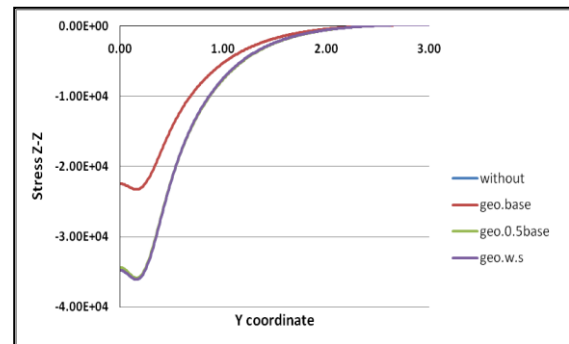


Fig. (22) Vertical stress σ_Z due to vertical pressure of wheel and friction force at bottom of base layer for sec. (A) with and without geosynthetics reinforcement

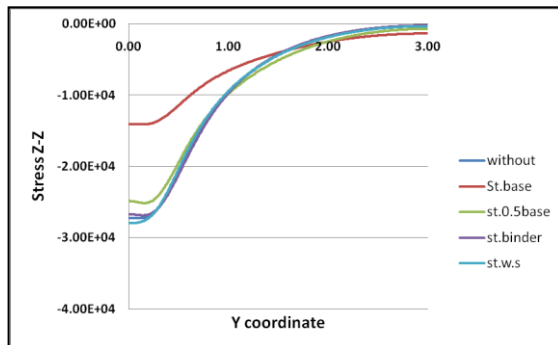


Fig. (23) Vertical stress σ_Z due to vertical pressure of wheel and friction force at bottom of base layer for sec. (B) with and without steel reinforcement

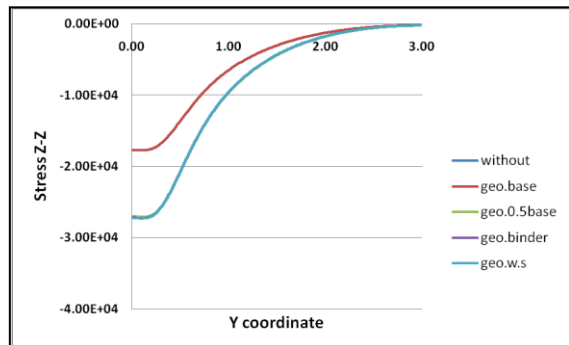


Fig. (24) Vertical stress σ_Z due to vertical pressure of wheel and friction force at bottom of base layer for sec. (B) with and without geosynthetics reinforcement

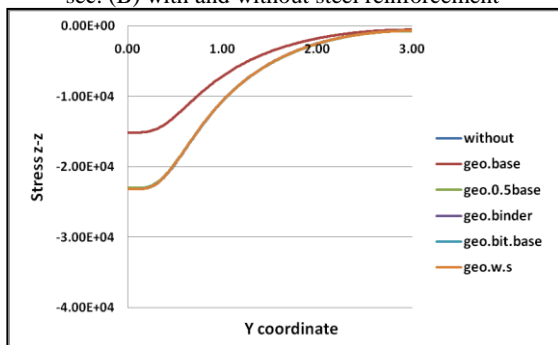


Fig. (25) Vertical stress σ_Z due to vertical pressure of wheel and friction force at bottom of base layer for sec. (C) with and without steel reinforcement

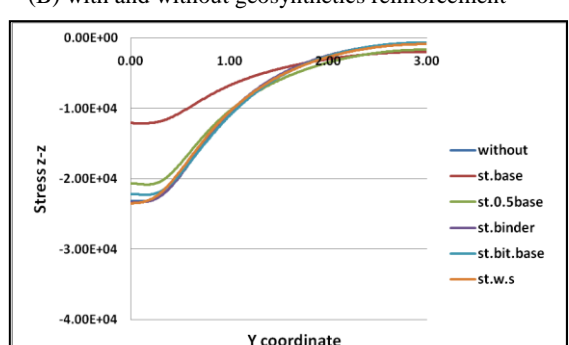


Fig. (26) Vertical stress σ_Z due to vertical pressure of wheel and friction force at bottom of base layer for sec. (C) with and without geosynthetics reinforcement

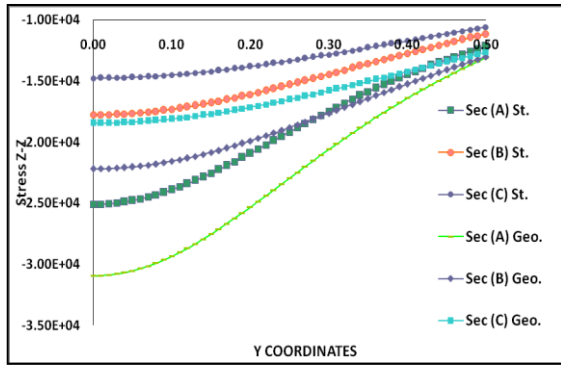


Fig. (27) Vertical stress σ_z due to vertical pressure of wheel at bottom of base layer for investigated sections with steel reinforcement or geosynthetics reinforcement

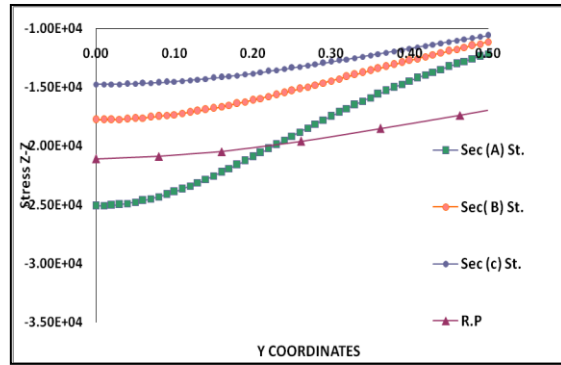


Fig. (28) Vertical stress σ_z due to vertical pressure of wheel at bottom of base layer for investigated sections with steel reinforcement or rigid pavement section

4.3.2 Lateral strain

Table (3) shows the values of lateral strain ϵ_Y under the centerline of the wheel load at top of subgrade for sections (A), (B) and (C) with steel or geosynthetic reinforcement and selected rigid pavement section 20cm reinforced concrete slab with steel diameter is 8 mm and rested on 15cm sub base layer. From this table it is clear that the values of lateral strain ϵ_Y in steel reinforced sections are decreased than its values in geosynthetic reinforced sections. Table also shows that the values of lateral strain ϵ_Y in rigid pavement section are lower with 7% than value in section (A) reinforced with steel but it is greater with 1.1% than values in sections (B) reinforced with steel and greater with 12.50% than the stress in section (C) reinforced with steel.

Table (3): Lateral strain ϵ_Y at top of subgrade due to vertical pressure of wheel for investigated sections with steel reinforcement or geosynthetics reinforcement and rigid pavement section

Reinforcement type	section	Lateral strain
Steel reinforcement	A	5.67E-05
	B	5.13E-05
	C	4.69E-05
Geosynthetics reinforcement	A	3.58E-04
	B	2.74E-04
	C	2.27E-04
Rigid pavement section		5.04E-05

V. CONCLUSIONS AND RECOMMENDATIONS

- 1- The best location for the reinforcement in all investigated flexible pavement sections is at the bottom of base layer.
- 2- In paving section cases subjected to vertical load due to wheel pressure only, the vertical stress σ_z under center line of wheel at bottom of base layer in steel wire grid reinforcement mesh cases is decreased by 48% from without reinforcement cases in paving sections (A), (B) and (C), while in geosynthetic reinforcement cases the decreasing percent is 35% from without reinforcement cases.
- 3- In the investigated three paving sections subjected to vertical load due to wheel pressure and horizontal friction force, the max vertical stress σ_z at bottom of base layer is located away from the center line of wheel by 0.17m. The vertical stress σ_z in steel wire grid reinforcement case is decreased by 48.75% from that without reinforcement cases in paving sections (A), (B) and (C), while in geosynthetic reinforcement cases the decreasing percent is about 36% from without reinforcement cases in the investigated sections.
- 4- The considered paving sections subjected to vertical load due to wheel pressure only, lateral strain ϵ_Y under the centerline of the wheel load at the bottom of base layer in steel wire grid reinforcement cases is

decreased from values in without reinforcement sections, by 86.70%, 83.60% and 81.50% for the investigated sections (A), (B) and (C) respectively, while in geosynthetic reinforcement cases the decreasing percents are 16%, 12.55% and 10.62% respectively.

- 5- When the paving sections subjected to vertical load as a result of wheel pressure and horizontal friction force, it is depicted the lateral strain ϵ_Y under the centerline of the wheel load at the bottom of base layer in steel wire grid reinforcement cases is decreased from without reinforcement sections by 83.00, 80.75% and 78.30% for the investigated sections (A), (B) and (C) respectively, while in geosynthetic reinforcement cases the decreasing percents are 10.8% in sections (A) and (B) while 8% for section (C).
- 6- Vertical stress σ_Z at top of subgrade in selected rigid pavement section is lower with 15.93% than value in section (A) reinforced with steel, but it is greater with 15.64% and 29.85% than values in sections (B) and (C) reinforced with steel respectively.
- 7- Lateral strain ϵ_Y under the centerline of the wheel load at top of subgrade in selected rigid pavement section is lower with 7% than value in section (A) reinforced with steel but it is greater with 1.1% and 12.50% than values in sections (B) and (C) reinforced with steel respectively.
- 8- Investigators recommend:
 - Modeling the paving sections in three dimensional finite elements.
 - An economic study to assess the benefit of using proposed strengthening technique.
 - Enhance the analysis to include the environmental effects on the reinforced paving sections.
 - Investigate the effect of dynamic loading on the reinforced paving sections.

REFERENCES

- [1] Cebon D. Handbook of vehicle-road interaction. Lisse, The netherland: Swets and Zeitlinger B.V.; 2000.
- [2] Gillespie TD, Karamihas SM. Heavy truck properties significant to pavement damage. Vehicle-road interaction in: kulakowski BT, editor. ASTM STP 1225. Philadelphia: American Society for testing and materials; 1994.p.52-63.
- [3] Uddin W, Zhang AH, Fernandez F. Finite element simulation of pavement discontinuities and dynamic load response. Transportation Research Record 1448. Washington (DC): TRB, National Research Council; 1994. p. 100-6.
- [4] Hadi MNS, Bodhinayake BC. Non linear finite element analysis of flexible pavements. Adv Eng Soft 2003; 34(3):657-62.
- [5] Huang YH. Pavement analysis and design. 2nd Ed. New Jersey: Pearson/Prentice-Hall; 2004.
- [6] Vuong, B.T. and Choi, X., 2009. Modelling of responses of road pavements containing. Reinforced materials. Contract Report for RTA-NSW. ARRB Group Ltd. (Unpublished).
- [7] Bassam Saad, Hani Mitri and Hormoz Poorooshasb. 3D FE Analysis of Flexible Pavement with Geosynthetic Reinforcement. Journal of transportation engineering © ASCE / MAY 2006.
- [8] H. Akbulut, K. Aslatas. Finite element analysis of stress distribution on bituminous pavement and failure mechanism. Materials and design 26(2005)383-387.
- [9] ADINA 8.7.3 Manuals (2005) ADINA R&D, Inc. Watertown, MA, USA.
- [10] Specifications of General Authority for Roads and Bridges, Egypt 1990
- [11] Egyptian Code for roads, part (4) Road construction materials and tests, Egypt 2008.